ORIGINAL ARTICLE

Cancer Science WILEY

Inhibitor library screening identifies ispinesib as a new potential chemotherapeutic agent for pancreatic cancers

Yoshiki Murase[1] | Hiroaki Ono[1] (iD) | Kosuke Ogawa[1] | Risa Yoshioka[1] |
Yoshiya Ishikawa[1] | Hiroki Ueda[1] | Keiichi Akahoshi[1] | Daisuke Ban[1] | Atsushi Kudo[1] |
Shinji Tanaka[2] (iD) | Minoru Tanabe[1]

[1]Department of Hepatobiliary and
Pancreatic Surgery, Graduate School
of Medicine, Tokyo Medical and Dental
University, Tokyo, Japan

[2]Division of Molecular Oncology, Graduate
School of Medicine, Tokyo Medical and
Dental University, Tokyo, Japan

Correspondence
Hiroaki Ono, Department of Hepatobiliary
and Pancreatic Surgery, Graduate School
of Medicine, Tokyo Medical and Dental
University, 1-5-45 Yushima, Bunkyo-ku,
Tokyo 113-8519, Japan.
Email: ono.msrg@tmd.ac.jp

Funding information
Japan Society for the Promotion of Science,
Grant/Award Number: 21K08769

Abstract

Screening custom-made libraries of inhibitors may reveal novel drugs for treating pancreatic cancer. In this manner, we identified ispinesib as a candidate and attempted to determine its clinical efficacy and the biological significance of its functional target Eg5 in pancreatic cancer. One hundred compounds in our library were screened for candidate drugs using cell cytotoxicity assays. Ispinesib was found to mediate effective antitumor effects in pancreatic cancer. The clinical significance of the expression of the ispinesib target Eg5 was investigated in 165 pancreatic cancer patients by immunohistochemical staining and in Eg5-positive pancreatic cancer patient-derived xenograft (PDX) mouse models. Patients with Eg5-positive tumors experienced significantly poorer clinical outcomes than those not expressing Eg5 (overall survival; $P < .01$, recurrence-free survival; $P < .01$). Ispinesib or Eg5 inhibition with specific siRNA significantly suppressed cell proliferation and induced apoptosis in pancreatic cancer cell lines. Mechanistically, ispinesib acted by inducing incomplete mitosis with nuclear disruption, resulting in multinucleated monoastral spindle cells. In the PDX mouse model, ispinesib dramatically reduced tumor growth relative to vehicle control (652.2 mm^3 vs 18.1 mm^3 in mean tumor volume, $P < .01$ by ANOVA; 545 mg vs 28 mg in tumor weight, $P < .01$, by ANOVA). Ispinesib, identified by inhibitor library screening, could be a promising novel therapeutic agent for pancreatic cancer. The expression of its target Eg5 is associated with poorer postoperative prognosis and is important for the clinical efficacy of ispinesib in pancreatic cancer.

KEYWORDS
chemotherapy, Eg5, inhibitor library, ispinesib, pancreatic cancer

1 | INTRODUCTION

Pancreatic cancer is a common highly lethal malignancy. There were approximately 459 000 new cases and 432 000 deaths worldwide in 2018.[1] Currently, it is the third leading cause of cancer-related mortality in the United States, with an estimated 45 000 deaths annually.[2] It is projected that pancreatic cancer will become the second leading cause of cancer-related mortality by 2030.[3] Despite the development of radical surgical treatments, only 10%-20% of patients with pancreatic cancer are diagnosed as having resectable tumors, and the majority of patients have unresectable tumors or metastatic disease at the initial diagnosis, with a 5-year overall survival (OS) rate of <10%.[4] Thus, systemic therapies are essential for the treatment of unresectable or metastatic pancreatic cancer.

Of the systemic chemotherapy regimens for pancreatic cancer, use of the nucleotide analogue gemcitabine (difluorodeoxycytidine) has been well established as first-line therapy since the evidence showing the ability to improve survival rates was reported in 1997.[5] More recently, combined chemotherapy regimens, such as gemcitabine plus nab-paclitaxel or 5-fluorouracil plus oxaliplatin and irinotecan, have been developed and play a central role in the treatment of advanced pancreatic cancer.[6,7] Nonetheless, even with these newer chemotherapies, the survival rate of pancreatic cancer patients is still markedly poorer than many other cancers.[2] Therefore, there is an urgent need to develop more effective chemotherapeutic agents for this disease. Most recently, several small molecule inhibitors have been developed, with different mechanisms of action, such as DNA damage response inhibition, as well as other modalities like immunotherapies or microenvironment-targeted inhibitors.[8-11] However, major survival benefits remain elusive in pancreatic cancer.

Hence, we first developed a custom-made inhibitor library screening protocol to identify useful potential new therapeutic targets and, in this way, we identified ispinesib as a novel inhibitor. We evaluated its pharmacological mechanism of action and assessed its clinical application using the patient-derived xenograft (PSX) mouse as a preclinical model. This study showed that ispinesib may be an effective therapeutic agent for pancreatic cancer.

2 | MATERIALS AND METHODS

2.1 | Materials

Anti–Eg5 antibody (ab51976) and anti–Pericentrin (ab220784) were obtained from Abcam. Anti–Cleaved Caspase3 (5A1E; #9664), anti–Cleaved poly ADP-ribose polymerase (PARP; D64E10; #5625), anti–Phospho-Histone H3 (Ser10; #9701), anti–Phospho-cdc2 (10A11; #4539), and GAPDH (D16H11; #5174) were obtained from Cell Signaling Technology. Anti–α-tubulin (T9026) was obtained from Sigma-Aldrich. All inhibitors in our custom-made library were compounds available from Selleck Chemicals (see Table S1). Monastrol was obtained from Selleck Chemicals and filanesib was from R&D Systems.

2.2 | Cell cultures

The human pancreatic cancer cell lines MIAPaCa2, PSN1, Panc1, and Hs766T were obtained from the ATCC. All cell lines were authenticated by STR DNA profiling, and all experiments were performed with mycoplasma-free cells. These cells were cultured in DMEM (Sigma-Aldrich), including 10% FBS (Wako Chemicals) and 1% penicillin/streptomycin (P/S) (Gibco) in a humidified 37°C, 5% CO_2 chamber.

All 165 primary pancreatic cancer samples were obtained during surgery from patients treated at Tokyo Medical and Dental University (Tokyo, Japan) between March 2005 and May 2018. Normal pancreatic tissues were obtained from surgical samples of 116 patients. Relevant clinicopathological data are provided in Table S2. With the approval of the Ethics Committees of the Faculty of Medicine in Tokyo Medical and Dental University (permission No. M2000-1080, G2017-018), written informed consent to have data from their medical records used in research was obtained from all patients. Patients were anonymously coded in accordance with ethical guidelines, as set out in the Declaration of Helsinki.

2.3 | Cell proliferation assay

Cells (5×10^3 per well) were seeded into 96-well plates and incubated at 37°C overnight. At 24, 48, and 72 hours after ispinesib treatment, cell numbers were evaluated by an assay based on a colorimetric water-soluble tetrazolium salt, WST-8 (Cell Counting Kit-8; Dojindo Molecular Technologies), as previously described.[12] The absorbance of each well was measured at 450 nm using an iMark Absorbance Microplate Reader (Bio-Rad Laboratories).

2.4 | Inhibitor library screening

Our custom-made inhibitor library consisting of 100 compounds was developed by integrating the Preclinical/Clinical Compound Library and Highly Selective Inhibitor Library (Selleck Chemicals). These 100 inhibitors have been designed and selected as having different targets affecting independent signaling pathways from the combined inhibitor libraries and are listed in Table S1. Cells (5×10^3 per well) were seeded into 96-well plates and incubated at 37°C overnight. Each of the 100 compounds was individually added to the cancer cells growing attached to the plates. After 72 hours, cytotoxicity was evaluated by the WST-8 assay as relative absorbance normalized to untreated control cells.

2.5 | Clonogenic survival assay

Long-term cell survival was evaluated by clonogenic survival assays as described.[12] In brief, cells (3×10^3 per well) were seeded into six-well plates in duplicate. After overnight incubation, attached cells

were treated with ispinesib (10 nmol/L) for 24 hours. Culture medium was subsequently changed to fresh medium without ispinesib. Cells were incubated for at least 1 week, and those growing as colonies were stained with 0.3% crystal violet solution. Cell occupancy was calculated using ImageQuant TL (GE Healthcare).

2.6 | Cell cycle analysis

After pancreatic cancer cells were treated with 10 nmol/L ispinesib for 48 hours, they were fixed in 70% ethanol at −20°C overnight. To evaluate the DNA content, cells were stained with 50 μg/mL propidium iodide (Sigma-Aldrich) with Triton X-100 and RNAase. The sample was subjected to flow cytometric analysis using FACS Canto II (BD Biosciences). Cell cycle analyses were conducted using FlowJo software (Tree Star).

2.7 | Quantitative real-time RT-PCR

Extracted RNA was reverse-transcribed into first-strand cDNA using SuperScript VILO cDNA Synthesis Kits (Invitrogen). Expression of mRNA was determined using TaqMan Gene Expression Assays (Applied Biosystems). The TaqMan assay used in this study was kinesin family member 11 (KIF11); Hs00189698_m1. Gene expression values are presented as ratios between genes of interest and an internal reference gene (Hs99999901_s1 for eukaryotic 18S) and subsequently normalized against the value for the control (relative expression level). Normal pancreas RNA (Human Adult Normal Tissue 5 Donor Pool: #R1234188-P) was purchased from BioChain Institution. Each assay was performed in duplicate for each sample.

2.8 | Western blotting

Western blotting was performed as previously described.[13] Protein bands were visualized with enhanced chemiluminescence using ImageQuant LAS 4000 mini (GE Healthcare). GAPDH was used as a loading control marker for normalization of each lane.

2.9 | Gene silencing by siRNA

Loss-of-function analysis was performed by siRNA targeting Eg5 (Invitrogen: Stealth RNAi-KIF11HSS105842 sense 5′-CCCAUC AACACUGGUAAGAACUGAA-3′, antisense 5′-UUCAGUUCUU ACCAGUGUUGAUGGG-3′). An alternative sequence of siRNA targeting Eg5 (Invitrogen: Stealth RNAi-KIF11HSS105843 sense 5′-GGAAACAGCCUGAGCUGUUAAUGAU-3′ antisense 5′-AUCAU UAACAGCUCAGGCUGUUUCC-3′) was used to exclude off-target effects of siRNA. Stealth RNAi siRNA Negative Control Lo GC (Invitrogen) was the negative control. Each siRNA (20 nmol/L) was transfected into cells using Lipofectamine RNA iMAX (Invitrogen),

according to the manufacturer's instructions. Knockdown of each target gene was confirmed by western blotting.

2.10 | Immunofluorescence staining

Cells were grown on four chamber CultureSlides (FALCON) and treated with 10 nmol/L ispinesib for 96 hours. The cells were fixed in 4% formaldehyde in PBS for 15 minutes, blocked with blocking buffer (PBS with 5% BSA and 0.2% Triton X-100) for 1 hour, and incubated overnight with the primary antibody at 4°C (anti–α-tubulin 1:500, anti–Pericentrin 1:1000, anti–Cleaved Caspase 3; 1:500). Alexa Fluor 594-conjugated goat anti–rabbit IgG antibodies and Alexa Fluor 488-conjugated goat anti–mouse IgG antibodies (#8889 and #4408, respectively; Cell Signaling Technology) were used as secondary antibodies (1:1000). The cells were viewed under a fluorescence microscope (BZ-700; KEYENCE and Leica DMi8; Leica microsystems).

2.11 | Immunohistochemistry

Indirect immunohistochemistry (IHC) was conducted on paraffin-embedded tissue sections of pancreatic ductal adenocarcinoma. Heat-induced epitope retrieval was carried out with 1 mmol/L EDTA buffer. After inactivation of endogenous peroxidase with 3% H_2O_2, the samples were incubated with 5% goat serum for 1 hour at room temperature to block nonspecific antibody binding. Anti–Eg5 antibody was diluted 1:500 with Signal stain antigen-antibody diluent (#8112; Cell Signaling Technology) and incubated overnight at 4°C in a moist chamber. Antigen-antibody reactions were detected with SignalStain (HRP, Mouse #8125; Cell Signaling Technology). At least 10 representative fields were examined for each sample, and the percentage of the total cell population that expressed Eg5 was calculated for each case. Expression of Eg5 protein was graded as either positive (≥10% of tumor cells showing immunopositivity) or negative (<10% of tumor cells stained, or no staining). This was independently assessed by two investigators. Paraffin-embedded samples of MIAPaCa2 cells and normal pancreatic tissues were used as positive and negative controls, respectively.

2.12 | Mouse xenograft model

Six-week-old male nude mice (Japan SLC) were injected subcutaneously in the left lower flank with MIAPaCa2 cells (7.5×10^6). For the patient-derived xenograft mouse model, 5-week-old female NSG mice (Charles River Laboratories Japan) were subcutaneously created by implanting a tumor with a diameter of 5 mm from a single pancreatic cancer patient according to a previous report.[14] Treatment was initiated when tumors were measurable (approximately 50–100 mm³). Mice were treated with ispinesib (10 mg/kg) or at different concentrations of ispinesib (1, 3, and 10 mg/kg) compared to

control vehicle (10% ethanol dissolved in PBS) by i.p. injection every 4 days. Tumor volumes were measured every 4 days and calculated using the following formula: volume = $1/2 \times$ length $\times$ width^2. All mouse procedures were approved by the Institutional Animal Care and Use Committee of Tokyo Medical and Dental University (permission No. A2019-263C2) and conducted under the relevant guidelines and regulations established by it.

2.13 | Statistical analysis

Clinicopathological features were compared using χ^2-tests or Fisher's exact tests for categorical variables. Survival probabilities were estimated using the Kaplan-Meier method and compared via log-rank tests. Significant variables were subjected to univariate and multivariate analysis using a Cox proportional hazards model. A $P < .05$ was considered statistically significant. Difference between subgroups were tested using Student's t test. For multiple group comparisons, ANOVA followed by Scheffé post-hoc testing or the Kruskal-Wallis test was used. All statistical analyses were performed using SPSS version 26.0 (SPSS).

3 | RESULTS

3.1 | Inhibitor screening identifies ispinesib as a new potential drug for pancreatic cancer

Here, we have established a custom-made inhibitor screening platform consisting of a library of 100 drugs by integrating the Preclinical/Clinical Compound Library and Highly Selective Inhibitor Library (from Selleck Chemicals). These 100 inhibitors had been designed and characterized as having different targets via independent signaling pathways (see Table S1 and Figure S1).

Using this library, we sought novel therapeutic agents for pancreatic cancer by screening cell growth inhibition. A fixed number of cancer cells seeded into 96-well plates was cultured with titrated amounts of each of the 100 compounds, and cell viability was measured after 72 hours by the WST-8 assay. Dose-response curves for each of the 100 drugs after 72 hours treatment are presented in Figure 1A, showing that although some of them lacked inhibitory effects at that time, most did inhibit proliferation of MIAPaCa2 and PSN1 cells. It was found that 21 drugs in the case of MIAPaCa2 and 26 for PSN1 inhibited proliferation by >50% compared to the vehicle control. Of these, we selected the top 20 with the greatest growth inhibitory effect. Based on the results of this drug screening approach using the two cell lines, nine drugs with inhibitory effects on both lines were selected as potential candidates for treating pancreatic cancer according to the scheme shown in Figure 1B.

The appropriate concentrations of these inhibitors were then further evaluated for their inhibitory effects on cell proliferation. Dose-response curves for all nine inhibitors on MIAPaCa2 cells are shown in Figure 1C. The half maximal inhibitory concentration (IC50) values of four of these drugs were above 1 μmol/L, indicating growth inhibition only at high concentrations (#29, Adavosertib; #30, CP-673451; #47, Rabusertib, and #81, SB225002). Excluding known potential drugs for pancreatic cancer by literature review, three novel candidates were finally selected from the nine for further testing (#3, Panobinostat; #16, SNS-032, and #24, Ispinesib), Subsequently, we determined the anti–proliferative effects of these three drugs in detail by dose-response analysis using three different pancreatic cancer cell lines (MIAPaCa2, PSN1, and Panc1) (Figure 1D). In thE current study, we decided to focus on ispinesib, which showed the strongest inhibitory effect on all three cell lines even at low concentrations.

3.2 | Ispinesib suppresses cell proliferation by inducing dysfunctional cell division in metaphase in pancreatic cancer cells

To evaluate the effects of ispinesib on pancreatic cancer cells, cell viability assays were performed using MIAPaCa2 and PSN1 cells. As shown in Figure 2A, ispinesib significantly decreased cancer cell proliferation in a dose-dependent manner. Furthermore, colony formation assays demonstrated that ispinesib maintained suppressive effects on the long-term growth of pancreatic cancer cells (Figure 2B).

To characterize the impact of ispinesib on cell cycle distribution, flow cytometry analysis was performed. The fraction of cells arrested in the G2-M phase was significantly increased 48 hours after the start of ispinesib administration compared to the DMSO vehicle control (Figure 2C). As a previous study had similarly demonstrated in breast cancer, we found that ispinesib, indeed, promotes cell growth inhibition of pancreatic cancer in association with G2 or M phase.[15] We then investigated the cell-cycle regulatory machinery associated with G2/M transition. At the G2/M boundary, the involvement of the cdc2/cyclin B complex is essential.[16,17] In particular, dephosphorylation of cdc2 at tyrosine 15 is a critical event during progression into mitosis.[18] We found that phosphorylated cdc2 (Tyr 15) was markedly decreased in all pancreatic cancer cell lines after ispinesib treatment, as shown by western blotting in Figure 2D. We also confirmed that phospho-H3 (Ser10) was activated on exposure to ispinesib, suggesting that cancer cells progressed into mitosis rather than arresting in the G2 phase.

We then assessed the effects of other Eg5 inhibitors on G2/M cell cycle distribution to evaluate if they were as effective as ispinesib treatment. Filanesib and monastrol have also been characterized as Eg5 inhibitors.[19] These agents we tested also inhibited cdc2 phosphorylation, increased histone H3 phosphorylation, and induced G2/M arrest at the same concentrations that effectively inhibited cancer cell growth in pancreatic cancer cells (5 nmol/L for filanesib and 100 μmol/L for monastrol) (Figure S2A-D).

Finally, immunofluorescence microscopy was carried out to evaluate the morphological characteristics of the ispinesib-treated cancer cells. Morphological changes resulting in the formation of
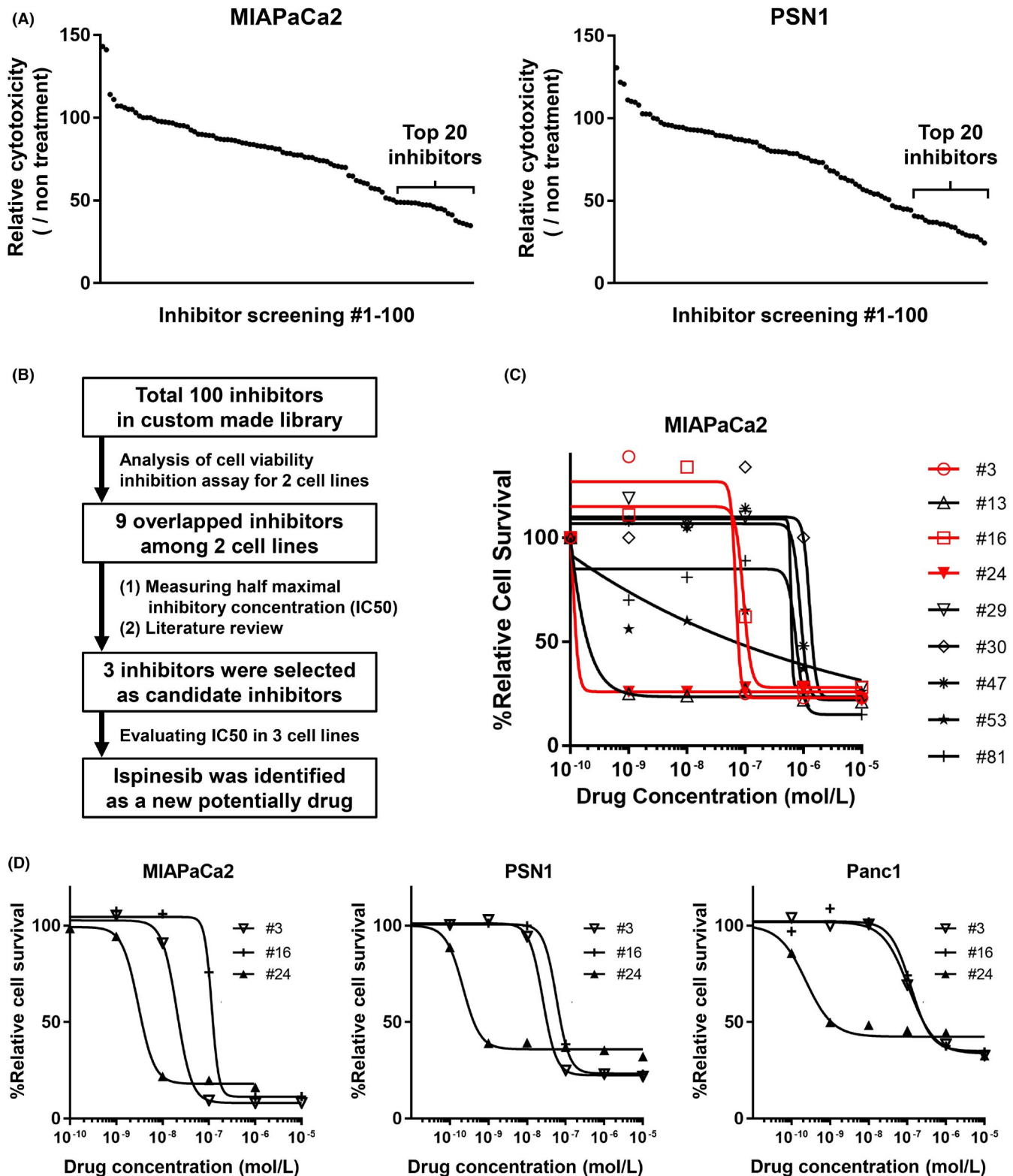
FIGURE 1 Identification of ispinesib from the 100 compounds in the drug library by pancreatic cancer cell screening. A, Dose-response curve for each of the 100 drugs on MIAPaCa2 and PSN1 cells. Each drug (10 μmol/L) was individually tested in 96-well plates compared to untreated controls by the WST-8 assay at 72 h. B, Overview of the inhibitor screening approach in two pancreatic cancer cell lines (MIAPaCa2 and PSN1). Nine drugs inhibiting both lines were identified within the top 20 inhibitors of both lines. After analyzing dose-response curves, and reviewing the literature, three drugs were selected as inhibitor candidates for further testing. C, Dose-response curves for nine inhibitors on MIAPaCa2 cells by the cytotoxicity assay. Four drugs were effective only at high concentrations (#29, #30, #47, and #81). One drug could not be assessed for IC50 (#53). Dose-response curves of the three candidate inhibitors is marked with a red line. D, Dose-response curves for three inhibitors (#3, #16, and #24) on pancreatic cancer cell lines (MIAPaCa2, PSN1, and Panc1). Of note, ispinesib was most effective even at low concentrations

multinucleated cancer cells were observed after ispinesib treatment, and mitotic cell division was particularly impaired. Multinucleated monoastral spindle cells were significantly induced by ispinesib treatment with up to a 10-fold increase relative to vehicle controls (Figure 2E).

3.3 | Ispinesib induces apoptosis in vitro and increases the anti–tumor effect in the xenograft model

Our results suggested that this morphological change was probably attributable to mitotic failure. Cell cycle arrest may be due to mitotic dysfunction and induction of cell death in cancer cells. Ispinesib treatment, indeed, increased Cleaved Caspase-3 and Cleaved PARP, indicating that this drug caused Caspase-dependent apoptosis of pancreatic cancer cells (Figure 3A). Furthermore, the characteristic morphological changes to these multinucleated cells and the activation of Cleaved Caspase-3 were also confirmed by immunofluorescence microscopy (Figure 3B). These results demonstrated that ispinesib forced the pancreatic cancer cells to progress into metaphase with inappropriate mitosis leading to apoptosis.

Experiments using mouse xenograft models were subsequently carried out to evaluate anti–tumor efficacy in vivo. Human pancreatic cancer xenografts were generated by subcutaneous implantation of MIAPaCa2 cells orthotopically into the flanks of nude mice. Tumor-bearing mice were then treated intraperitoneally with ispinesib or control vehicle for 3 weeks, six times every 4 days after the start of treatment and followed up for 48 days. As shown in Figure 3C, the volume of subcutaneous tumors was significantly reduced by ispinesib treatment comparing to vehicle controls (1112.7 mm^3 vs 131.9 mm^3 mean tumor volume, $P < .01$ by ANOVA, 840 mg vs 95 mg tumor weight, $P < .01$, by ANOVA). The dose-dependent anti–tumor efficacy of ispinesib was also evaluated (Figure 3D). Tumor growth was significantly inhibited by 3 mg/kg of ispinesib. Furthermore, 10 mg/kg dose treatment inhibited tumor growth more markedly, demonstrating a dose-dependent inhibitory effect of ispinesib treatment (tumor volume and tumor weight, $P < .01$, by Kruskal-Wallis
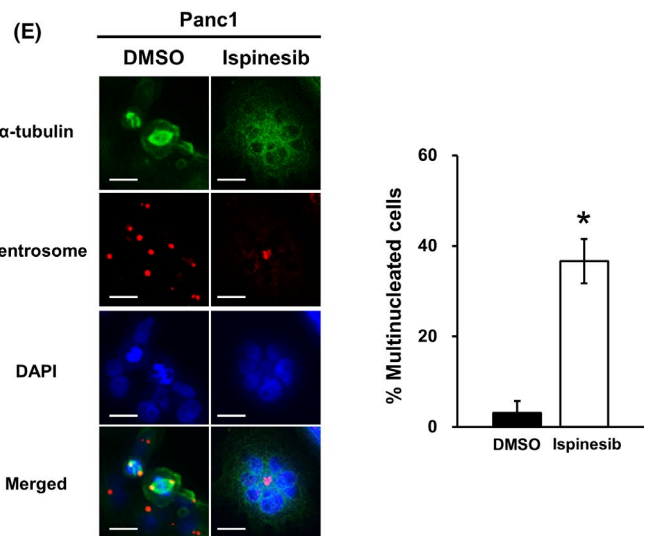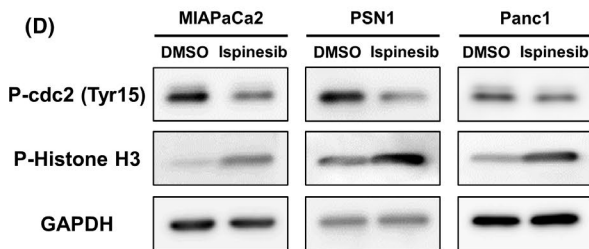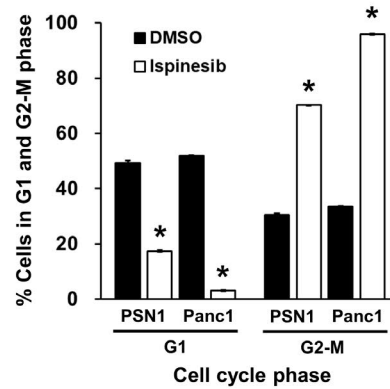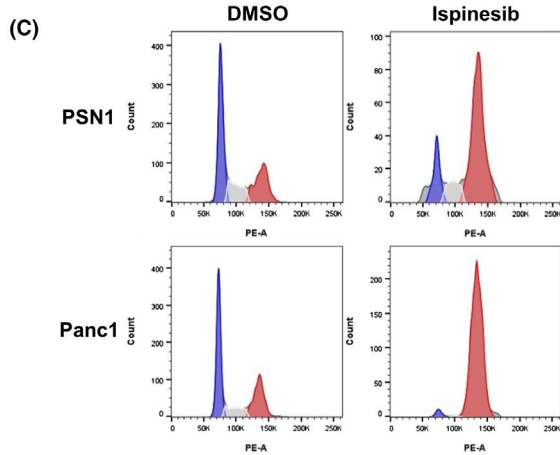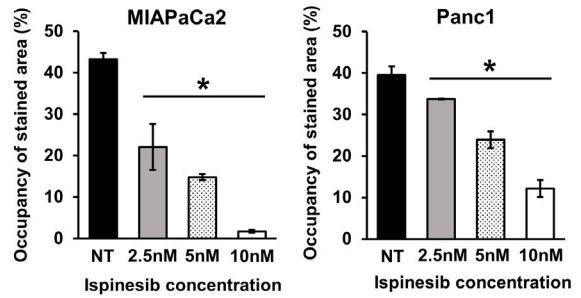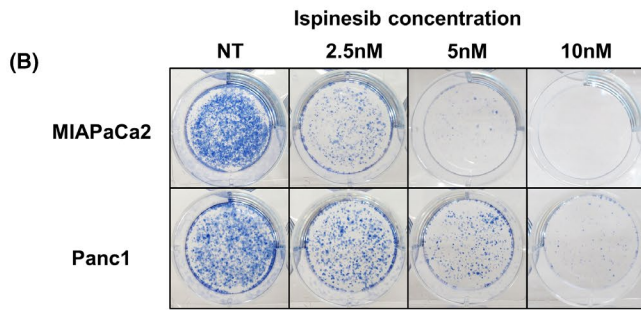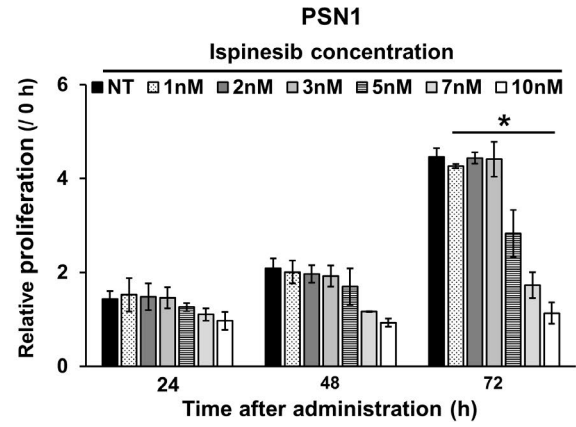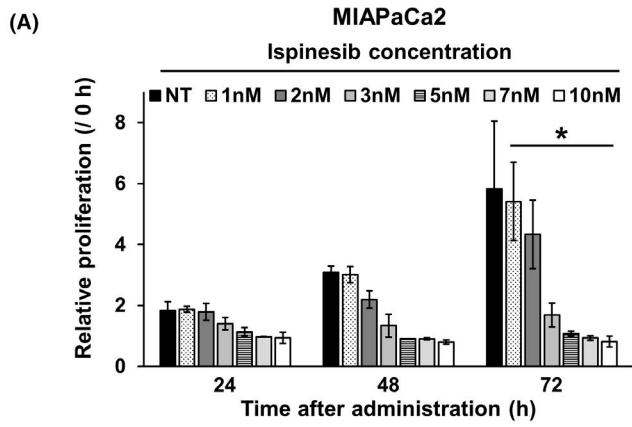
test). Representative images of the tumors performed in these mouse xenograft experiments are shown in Figure S3A,B.

3.4 | Eg5 is the functional target of ispinesib in pancreatic cancer cells

The kinesin-like spindle protein Eg5 plays an essential role in establishing a bipolar spindle during mitosis. Ispinesib was designed as a functional inhibitor of Eg5.[20,21] It binds to Eg5 and creates a protein complex with extensive hydrophobic interactions, suggesting that ispinesib functions as an allosteric inhibitor. Thus, whether Eg5 is expressed in pancreatic cancer cells would be predicted to be an important restriction on the clinical efficacy of ispinesib. The biological significance of Eg5 in pancreatic cancer has not been determined so far. Therefore, we quantified Eg5 expression in a panel of pancreatic cancer cell lines. Western blotting analysis revealed that Eg5 protein was present in all available pancreatic cancer cell lines. Furthermore, quantitative RT-PCR analysis demonstrated that Eg5 mRNA expression was aberrantly increased 5 to 10-fold higher than in normal pancreatic tissue, suggesting that Eg5 presents a cancer-specific expression pattern (Figure 4A,B).

We subsequently evaluated the biological effects of Eg5 to clarify the function of ispinesib using specific siRNA targeting Eg5. Effective knockdown of Eg5 was confirmed by western blotting in these cells (Figure S4A). WST-8 cell viability assays demonstrated that Eg5 siRNA treatment suppressed the proliferation of MIAPaCa2, PSN1, and Panc1 cells (Figure 4C). The proportion of cells accumulating in the G2-M phase was significantly increased by Eg5-specific-siRNA compared with negative control siRNA transfected into PSN1 or Panc1 cells. Reciprocally, cells in the G1 phase were markedly decreased (Figure 4D). Cleaved Caspase-3 and PARP were activated in cells transfected with Eg5-specific siRNA after 72 hours in MIAPaCa2 and PSN1 cells and after 96 hours in Panc1 cells (Figure 4E). Cleaved Caspase-3 activation was also identified by immunofluorescence staining (Figure S4B). Eg5-induced cell growth inhibition, cell cycle arrest in the G2/M phase, and cell death mediated through caspase-dependent apoptosis by virtue of its inhibitory

---

FIGURE 2 A, Dose-response characteristics for ispinesib on MIAPaCa2 and PSN1 cells. Cancer cells (5 × 10^3 cells per well) were seeded into 96-well plates and treated with ispinesib at each concentration (1-10 nmol/L) for different periods of time (24-72 h). Ispinesib significantly suppressed cell proliferation in a dose-dependent manner. Each experiment was performed in duplicate. Error bars represent mean ± standard deviation (SD). *$P < .05$ by one-way ANOVA with post-hoc Scheffé test. B, Left panel, representative image of clonogenic cell survival assays with different doses of ispinesib, using MIAPaCa2 and Panc1 cells. Right panel, occupancy of the stained colony area was evaluated in MIAPaCa2 and Panc1 cells. The ability to form colonies after ispinesib treatment was significantly decreased in both cell lines. Error bars represent mean ± SD. *$P < .05$ by one-way ANOVA with post-hoc Scheffé test. C, Effect of ispinesib on cell cycle stage. Flow cytometry was performed after 10 nmol/L ispinesib treatment of PSN1 and Panc1 cells for 48 h. Ispinesib treatment significantly increased the fraction of cells arrested in the G2-M phase, whereas the fraction of cells in the G1 phase was decreased. Experiments were performed in duplicate. Error bars represent mean ± SD. *$P < .05$ vs DMSO control vehicle by student t test. D, Western blotting of Phospho-Histone H3 (Ser10) and Phospho-cdc2 (Tyr15) after ispinesib treatment (10 nmol/L) for 72 h. Notably, Phospho-Histone H3 was increased and Phospho-cdc2 (Tyr15) decreased in all pancreatic cancer cell lines (MIAPaCa2, PSN1, and Panc1) in response to ispinesib treatment. E, Immunofluorescence staining after ispinesib treatment of Panc1 cells. Characteristic morphology, such as cell swelling, multinucleation, and monoastral spindles, was observed in the ispinesib-treated cells. When treated with ispinesib, the proportion of multinucleated cells (44.9%) was significantly increased relative to vehicle control (4.1%). In contrast, normal bipolar spindles were observed in DMSO vehicle-treated cells. Error bars represent mean ± SD. *$P < .01$ vs vehicle control by Student t test. Bars, 20 μm

(A) MIAPaCa2 / PSN1 — Relative proliferation (/0 h) vs Time after administration (h) for Ispinesib concentrations NT, 1nM, 2nM, 3nM, 5nM, 7nM, 10nM

(B) Ispinesib concentration: NT, 2.5nM, 5nM, 10nM for MIAPaCa2 and Panc1; Occupancy of stained area (%)

(C) PSN1 and Panc1 cell cycle analysis (DMSO vs Ispinesib); % Cells in G1 and G2-M phase

(D) MIAPaCa2, PSN1, Panc1 western blots (DMSO vs Ispinesib): P-cdc2 (Tyr15), P-Histone H3, GAPDH

(E) Panc1 (DMSO vs Ispinesib): α-tubulin, Centrosome, DAPI, Merged; % Multinucleated cells

mechanism shown using Eg5-siRNA. Thus, we have confirmed that these results are similar to those obtained with ispinesib treatment.

3.5 | Clinical significance of Eg5 expression and therapeutic application of ipsinesib for pancreatic cancer patients

To investigate the clinicopathological significance of Eg5 expression, we conducted an immunohistochemical analysis of 165 surgically resected cases of pancreatic cancer. Notably, Eg5 was expressed in 116 of them (70.3%) (Figure 5A). In contrast, Eg5 expression was not identified in any normal pancreatic tissues. Immunostaining for Eg5 was identical with the mRNA expression results and also represents a cancer-specific expression pattern. Regarding clinicopathological characteristics, it was found that Eg5-positivity was significantly associated with extra-pancreatic and venous invasion ($P = .001$ and .011, respectively; Table S2.)

Next, we assessed associations between Eg5 expression and postoperative prognosis. OS and recurrence-free survival (RFS) revealed a significant association between Eg5-positivity and poorer survival by Kaplan-Meier analysis with log-rank testing (median OS: 20.9 months vs 69.1 months; $P < .01$ and median RFS: 10.8 months vs 30.4 months; $P < .01$, respectively; Figure 5B).

In univariate analysis, Eg5-positivity, carcinoembryonic antigen (CEA), carbohydrate antigen 19-9 (CA19-9), surgical procedure, tumor size, extra pancreatic invasion, residual tumor, venous invasion, neural invasion, lymphatic invasion, T status, and N status were significantly associated with OS according to the Cox proportional hazards regression model. By multivariate analysis using a simultaneous procedure, Eg5-positivity, CEA, and residual tumor remained independent predictive factors for OS (Table 1).

Finally, we performed further in vivo experiments to test the clinical application of ispinesib for pancreatic cancer patients. Patient-derived mouse xenograft (PDX) models were generated by transplanting surgically removed tumor cells from a single cancer patient under the skin of mice. A strength of this mouse model is that the tumor is implanted along with the surrounding tissue, so that the tumor microenvironment more closely resembles the actual in vivo environment in the patient. Therefore, the PDX mouse model makes

it possible to verify therapeutic outcomes more effectively than in a conventional mouse model.[22] We have successfully generated PDX mice using surgical specimens of invasive pancreatic cancer and have evaluated the therapeutic outcome of ispinesib treatment in this model.

Prior to the initiation of ispinesib treatment, the Eg5-positivity of the primary cancer tissues of the patient used to generate the PDX model was confirmed by immunohistochemical staining (Figure S5A). Mice bearing the tumor were treated with ispinesib every 4 days for 4 weeks (total eight times). Ispinesib dramatically reduced the volume of subcutaneous tumors relative to vehicle control (652.2 mm^3 vs 18.1 mm^3 mean tumor volume, $P < .01$ by ANOVA; 545 mg vs 28 mg tumor weight, $P < .01$, by ANOVA), as shown in Figure 5C. Representative images of the tumors in the PDX model are shown in Figure S5B. As shown in Figure 5D, Eg5 expression was also confirmed in the tumor of the PDX model mice. This clearly demonstrates the clinical efficacy of ispinesib for Eg5-positive pancreatic cancer.

4 | DISCUSSION

A custom-made drug library screening method combining two commercially available libraries was exploited in the current study. A total of 100 compounds with unique targets based on their inhibitory effects on different signaling pathways was screened to identify potential novel therapeutic agents for pancreatic cancer. Using this screening approach, three compounds were identified as candidate drugs inhibiting the proliferation of pancreatic cancer cells. Of these, we focused on ispinesib as the most active in inhibiting cell proliferation by inducing G2/M cell cycle arrest and ultimately promoting apoptosis. In particular, mechanistically, ispinesib caused cell cycle arrest accompanied by characteristic mitotic failure in pancreatic cancer cells, as shown in Figure 2E. Thus, ispinesib causes G2/M cell cycle arrest with incomplete mitosis and induces apoptosis of pancreatic cancer cells.

When cell division functions normally, bipolar spindles are formed during mitosis. In contrast, as shown in Figure 2E, unipolar spindles, especially those characterized as monoastral spindle formations, were observed with inappropriate mitosis after cancer cells

---

FIGURE 3 A, The apoptosis markers Cleaved Caspase-3 and PARP are increased in MIAPaCa2 and PSN1 cells after 72 h and Panc1 cells after 96 h of ispinesib treatment (10 nmol/L) as assessed by Western blotting. B, Representative images of immunofluorescence staining of Cleaved Caspase-3 in MIAPaCa2 and Panc1 cells. Cleaved Caspase-3 was increased, accompanied by changes to multipolar or multinucleated morphology after exposure to ispinesib (10 nmol/L) for 72 h to MIAPaCa2 and for 96 h to Panc1. Bars, 50 μm. C, Antitumor activity of ispinesib for xenografted pancreatic tumors in nude mice. Mice were inoculated with MIAPaCa2 cells (7.5×10^6) in their flanks by subcutaneous injection. Once tumors reached measurable size, ispinesib (10 mg/kg) or control vehicle was injected i.p. according to a q4d × 6 schedule (ispinesib and control vehicle; each N = 8). The volume of the tumors was recorded over the 48 d of ispinesib treatment. Arrows indicate the days of ispinesib administration. Representative images of xenografted tumors in mice at necropsy and the weights of these tumors are also shown. Of note, ispinesib treatment significantly inhibited tumor growth (*$P < .01$ by one-way ANOVA with post-hoc Scheffé test). Error bars represent mean ± SD. D, The dose-dependent mouse xenograft experiment of ispinesib. The dose of ispinesib was set to 1, 3, and 10 mg/kg (ispinesib and control vehicle; each N = 4). Arrows indicate the days of ispinesib administration. Representative images of xenografted tumors and the weights and volume of these tumors at necropsy are shown. Ispinesib treatment significantly inhibited tumor growth in a dose-dependent manner (P-values by Kruskal-Wallis test). Error bars represent mean ± SD

(A)

(B)

(C)

(D)
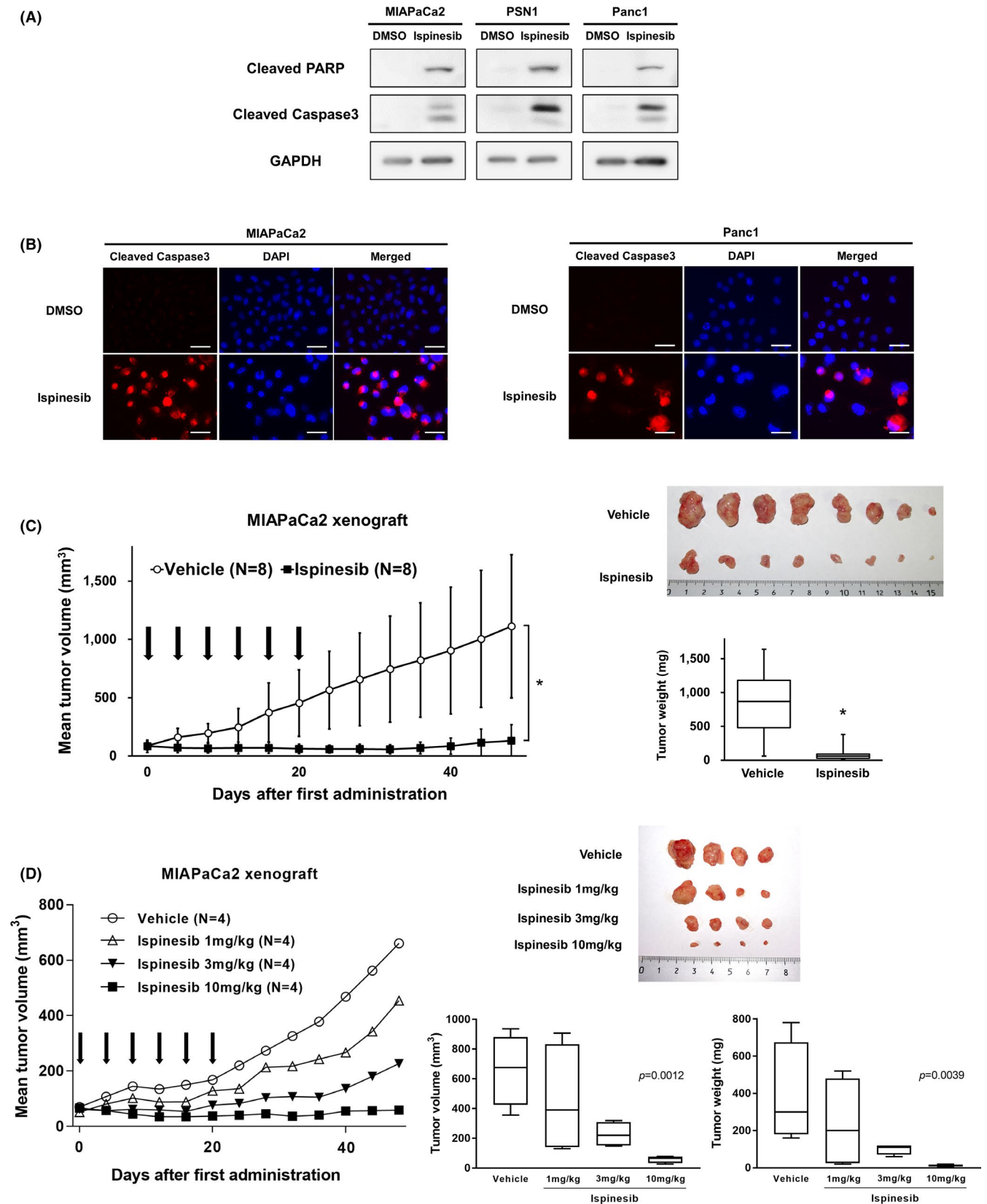
were exposed to ispinesib. Eg5 is known to be a functional target for ispinesib. This characteristic cell morphology was also observed during Eg5 suppression, as verified by specific inhibition using Eg5-targeting siRNA (Figure 4D,E). The inhibitory effect of ispinesib and Eg5 suppression on cell proliferation in pancreatic cancer cells was mainly due to the characteristic mechanism of mitosis failure.
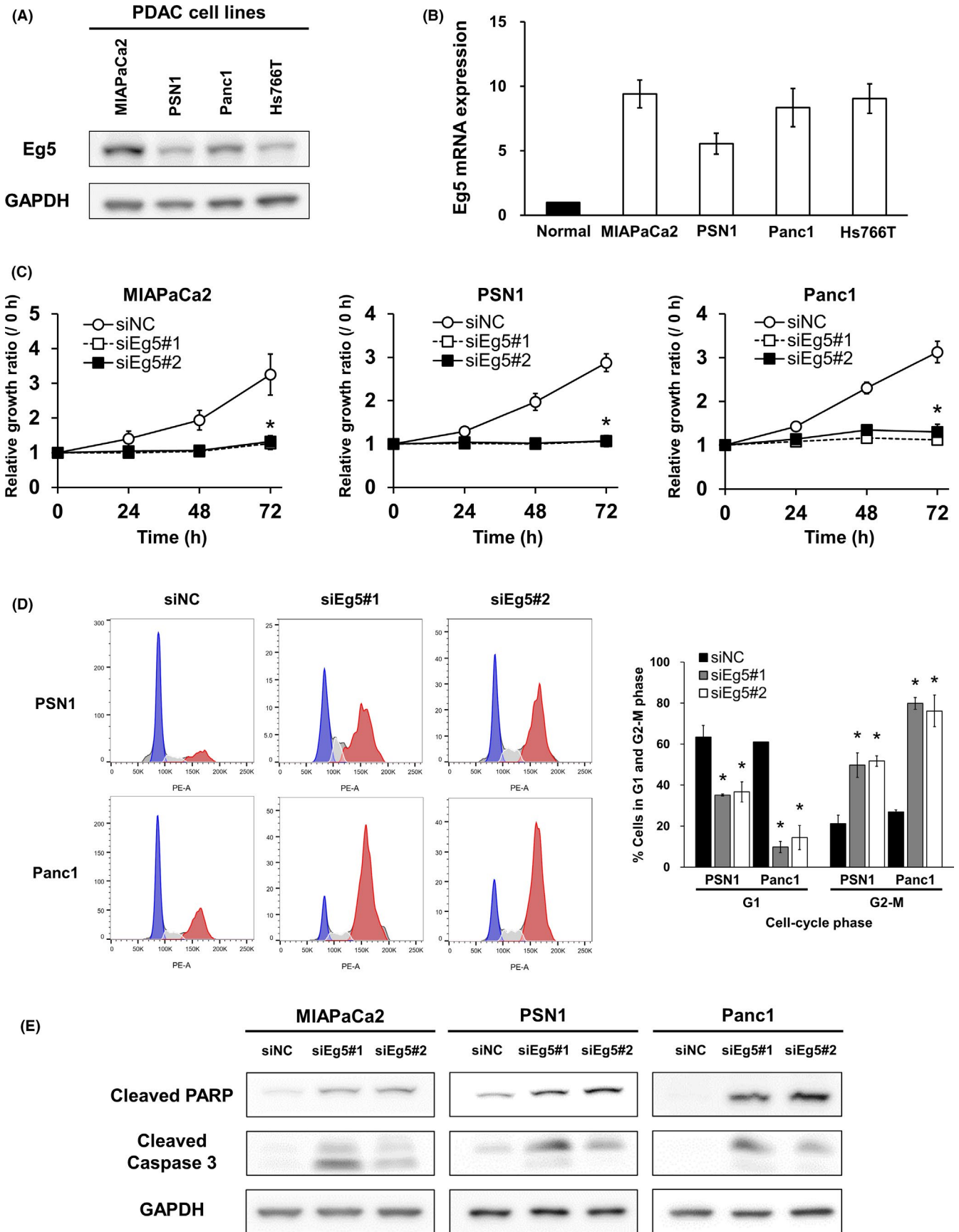
FIGURE 4 A, Endogenous Eg5 protein expression in pancreatic cancer cell lines (MIAPaCa2, PSN1, Panc1, and Hs766T) by western blotting. Eg5 expression was observed in all 4 pancreatic cancer cell lines. B, Endogenous Eg5 mRNA expression in pancreatic cancer cell lines. Quantitative RT-PCR showed that Eg5 expression elevated 5 to 10-fold in pancreatic cancer cell lines compared to normal pancreatic tissues. C, Effect of Eg5 gene-silencing on proliferation of MIAPaCa2, PSN1, and Panc1 cells. Cell proliferation was evaluated from 24 to 72 h. The proliferative activity of pancreatic cancer cells was significantly suppressed by Eg5-specific siRNA compared to negative control siRNA. Error bars represent mean $\pm$ SD. *$P < .05$ vs negative control siRNA-treated cells by one-way ANOVA with post-hoc Scheffé test. Each data point was evaluated as relative absorbance normalized to negative control siRNA. Each experiment was performed in triplicate. D, Effect of Eg5 gene-silencing on cell cycle distribution. Cell cycle distribution was analyzed after Eg5 siRNA transfection at 48 h. The population in each phase of the cell cycle (left) and quantified cell cycle distribution (right) in PSN1 and Panc1 cells is shown. Eg5 gene-silencing significantly increased the fraction of cells arresting in G2-M, whereas the fraction of cells in G1 was decreased. Error bars represent mean $\pm$ SD. *$P < .05$ vs negative control siRNA by student t test. Each experiment was performed in triplicate. E, The apoptosis markers Cleaved Caspase-3 and PARP were increased in Eg5 siRNA-treated MIAPaCa2, PSN1 and Panc1 cells for 72 h compared to negative control siRNA, as assessed by Western blotting

Eg5 (also known as KIF11) is a mitotic spindle kinesin and is a member of a superfamily of molecular motors that are relevant for a variety of cellular functions, with important roles in motility, such as cytoplasmic transport and mitosis formation.[23,24] Eg5 is functionally involved in the separation of duplicated centrosomes in spindle formation to establish a bipolar mitotic spindle.[23] In cancer cells, overexpression of Eg5 causes genetic instability and is associated with poorer prognosis in a mouse model.[25] Thus, there is increasing evidence that Eg5 expression may be biologically linked to the cancer phenotype and constitutes a potential drug target for the development of novel cancer chemotherapeutic agents. In this study, we further confirmed the inhibitory effect on cell proliferation in pancreatic cancer cells using several Eg5 inhibitors, including monastrol and filanesib, in addition to ispinesib (Figure S2A-D).

Mechanistically, Eg5 binds to ispinesib to form a complex, leading to a conformational change in the Eg5 structure itself. Ispinesib induces a loop change in Eg5, which regulates the conformation of both the ATP-binding site and the mechanical elements of the force-generating motor.[26] Ispinesib acts as an allosteric inhibitor by interacting with the binding pocket of Eg5 through hydrophobic interactions.[20] Based on the mechanism of action, monastrol and filanesib are classified as similar Eg5 inhibitors.[19] Compared to monastrol, the inhibitory effect of cell proliferation was sufficiently achieved at 5 nmol/L by filanesib. IC50 and inhibition of cell proliferation were almost the equivalent between Filanesib and Ispinesib. Furthermore, it was common that they induced G2/M arrest (Figure S2A-D). These results were similar to the study comparing filanesib and ispinesib reported by Jungwirth G et al in meningioma cells.[27]

In relation to the structural mechanism, the level of expression of Eg5 is, therefore, important for the therapeutic efficacy of ispinesib. In earlier work, Eg5 was reported to be highly expressed in several malignant tumors, including pancreatic cancer.[28-32] Liu et al[29] reported that approximately 90% of pancreatic cancer specimens showed moderate to high Eg5 expression, while normal pancreatic cells had lower Eg5 expression. Their findings are in close agreement with ours, implying cancer-specific aberrant upregulation of Eg5. We further demonstrated that Eg5 expression is significantly associated with worse postoperative prognosis of pancreatic cancer patients (Figure 5B).

Evidence has been accumulating on the clinical efficacy of ispinesib in a variety of cancers, such as breast cancer. Recently, phase I/II trials for the evaluation of ispinesib have been conducted for several different cancers.[33-39] In terms of the clinical efficacy of ispinesib, 6.7% of patients with breast cancer achieved a partial response,[33] and 46% of patients with hepatocellular carcinoma reached a state of stable disease[37] based on the Response Evaluation Criteria In Solid Tumors (RECIST). It appears that the clinical anti–tumor effect of this inhibitor is not as marked as might be expected from the preclinical data. This may be at least partly due to the lack of appropriate preclinical models that can reproduce the characteristic feature of malignant tumors to assist in developing efficient drugs, evaluate the biological behavior of cancer, and overcome issues related to treatment effectiveness. The PDX mouse model may contribute to improved predictability of outcomes and prognosis more than conventional mouse models.[22] This model may, thus, help to predict the results of human clinical trials more accurately. Here, we report the generation of a PDX mouse model using surgical specimens of a patient with advanced pancreatic cancer and have evaluated the clinical efficacy of ispinesib in this preclinical model.

The clinical efficacy of ispinesib depends on whether Eg5 is expressed at sufficient levels in pancreatic cancer cells. Ispinesib is expected to be effective in patients with high Eg5 expression. As shown in the example in Figure 5A, Eg5 expression may be seen in up to 70% of the tumor cells in pancreatic cancer patients. In this study, we first confirmed by immunohistochemistry staining that the surgical specimens from the pancreatic cancer patient used to generate the PDX mouse model expressed high levels of Eg5. Thereafter, we used the model to confirm the clinical effects of ispinesib on the tumor. This would allow validation of the therapeutic effect before administering the drug to individual patients, reaffirming that this model is appropriate for preclinical testing. Thus, we documented the importance of Eg5 expression for the therapeutic effect of ispinesib.

In conclusion, using a custom-made inhibitor library, we have identified ispinesib as a drug with inhibitory effects on the proliferation of pancreatic cancer cells. Based on our evaluation in vitro and vivo, ispinesib induced apoptosis through inducing dysfunctional
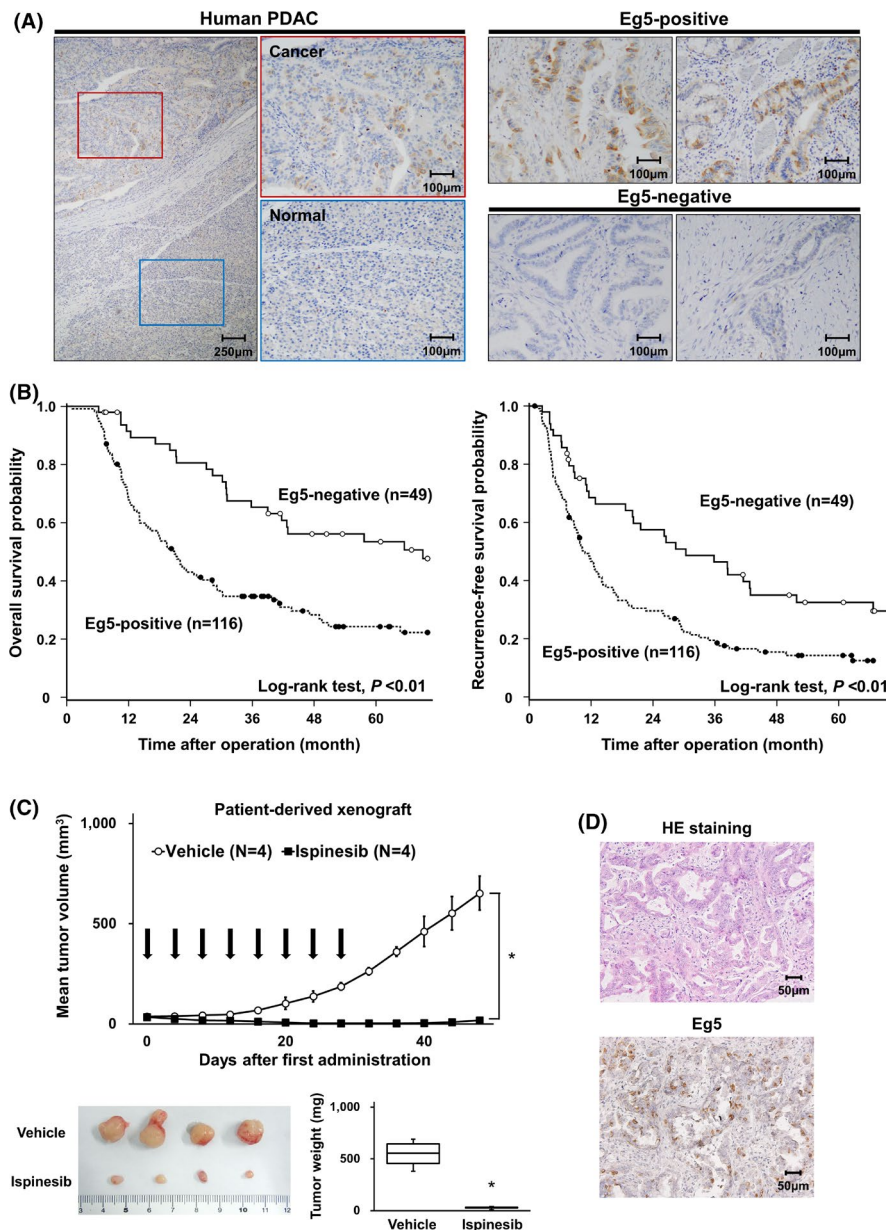
FIGURE 5 A, Left, representative immunohistochemical staining of Eg5 protein in normal pancreatic tissues and pancreatic cancer tissues. Right, representative negative and positive immunohistochemical staining of Eg5. Expression of Eg5 protein was graded as either positive (≥10% of tumor cells positive) or negative (<10% of tumor cells positive, or no staining). Paraffin-embedded samples of MIAPaCa2 cell and normal pancreatic tissues were used as the positive and negative control, respectively. B, Kaplan-Meier curves for overall survival (left) and recurrence-free survival (right) of 165 pancreatic cancer patients after surgical resection. Eg5-positivity by immunohistochemistry was significantly associated with worse overall and recurrence-free survival ($P < .01$; log-rank test). C, Antitumor activity of ispinesib in patient-derived xenografted nude mice. Ispinesib (10 mg/kg) was injected i.p. according to a q4d × 8 schedule. The volumes of the tumors were recorded over the 48 days of ispinesib treatment. Arrows indicate the days of ispinesib administration. Representative images of xenografted tumors in mice at necropsy, and the weight of these tumors is shown. Tumor growth was significantly inhibited by ispinesib treatment (*$P < .01$ by one-way ANOVA with post-hoc Scheffé test). Error bars represent mean ± SD. D, Representative images of H&E staining and immunohistochemical staining of Eg5 expression of tumors in the PDX mouse

cell division, suggesting that it has potential as a new therapeutic agent. High expression of Eg5, a target gene of ispinesib, is a poor prognostic factor for pancreatic cancer, and its expression would be a necessary requirement for indicating administration of the drug to patients in the clinical setting. The most advanced Eg5-targeting agent is ispinesib, which exhibits potent anti–tumor activity as shown in our study, indicating its potential as a novel therapeutic agent in pancreatic cancer.

TABLE 1 Cox proportional hazard regression analysis for overall survival

Characteristics	Category	Univariate analysis HR (95% CI)	P-value*	Multivariate analysis[a] HR (95% CI)	P-value*
Age	>70	1.32 (0.90-1.94)	.154	–	–
Sex	Male	0.89 (0.61-1.32)	.571	–	–
CEA, ng/mL	>5	1.67 (1.12-2.48)	**.012**	1.69 (1.10-2.59)	**.016**
CA19-9, U/mL	>100	1.70 (1.16-2.50)	**.007**	1.12 (0.75-1.68)	.579
Surgical procedure	PD	1.54 (1.01-2.34)	**.044**	–	–
Tumor size, mm	>30	1.64 (1.12-2.41)	**.012**	–	–
Extrapancreatic invasion	Positive	5.02 (2.04-12.4)	**<.001**	1.85 (0.69-4.93)	.219
Residual tumor	Positive	1.82 (1.21-2.73)	**.004**	1.96 (1.24-3.08)	**.004**
Venous invasion	Positive	5.21 (1.28-21.1)	**.021**	1.73 (0.40-7.42)	.460
Neural invasion	Positive	4.76 (1.51-15.0)	**.008**	–	–
Lymphatic invasion	Positive	2.44 (1.55-3.86)	**<.001**	1.47 (0.89-2.44)	.134
T status (UICC 8th)	≥T3	1.73 (1.15-2.61)	**.008**	1.34 (0.88-2.05)	.172
N status (UICC 8th)	≥N1	2.06 (1.37-3.11)	**.001**	1.36 (0.87-2.11)	.173
Eg5 expression	Positive	2.43 (1.52-3.88)	**<.001**	2.36 (1.45-3.84)	**.001**

Note: Statistically significant values are in bold type.

CA19-9, carbohydrate antigen 19-9; CEA, carcinoembryonic antigen; CEA, carcinoembryonic antigen; CI, confidence interval; HR, hazard ratio; UICC, Union for International Cancer Control.
[a]Simultaneous analyses were used for multivariate analysis. *P < .05.

REFERENCES
1. Bray F, Ferlay J, Soerjomataram I, Siegel RL, Torre LA, Jemal A. Global cancer statistics 2018: GLOBOCAN estimates of incidence and mortality worldwide for 36 cancers in 185 countries. *CA Cancer J Clin*. 2018;68:394-424.
2. Siegel RL, Miller KD, Jemal A. Cancer statistics, 2020. *CA Cancer J Clin*. 2020;70:7-30.
3. Rahib L, Smith BD, Aizenberg R, Rosenzweig AB, Fleshman JM, Matrisian LM. Projecting cancer incidence and deaths to 2030: the unexpected burden of thyroid, liver, and pancreas cancers in the United States. *Cancer Res*. 2014;74:2913-2921.
4. Gillen S, Schuster T, Meyer Zum Buschenfelde C, Friess H, Kleeff J. Preoperative/neoadjuvant therapy in pancreatic cancer: a systematic review and meta-analysis of response and resection percentages. *PLoS Med*. 2010;7:e1000267.
5. Burris HA, Moore MJ, Andersen J, et al. Improvements in survival and clinical benefit with gemcitabine as first-line therapy for patients with advanced pancreas cancer: a randomized trial. *J Clin Oncol*. 1997;15:2403-2413.
6. Conroy T, Desseigne F, Ychou M, et al. FOLFIRINOX versus gemcitabine for metastatic pancreatic cancer. *N Engl J Med*. 2011;364:1817-1825.
7. Von Hoff DD, Ervin T, Arena FP, et al. Increased survival in pancreatic cancer with nab-paclitaxel plus gemcitabine. *N Engl J Med*. 2013;369:1691-1703.
8. Mateo J, Lord CJ, Serra V, et al. A decade of clinical development of PARP inhibitors in perspective. *Ann Oncol*. 2019;30: 1437-1447.
9. Bear AS, Vonderheide RH, O'Hara MH. Challenges and opportunities for pancreatic cancer immunotherapy. *Cancer Cell*. 2020;38:788-802.
10. Mizrahi JD, Surana R, Valle JW, Shroff RT. Pancreatic cancer. *Lancet*. 2020;395:2008-2020.
11. Ho WJ, Jaffee EM, Zheng L. The tumour microenvironment in pancreatic cancer – clinical challenges and opportunities. *Nat Rev Clin Oncol*. 2020;17:527-540.

12. Ono H, Basson MD, Ito H. P300 inhibition enhances gemcitabine-induced apoptosis of pancreatic cancer. *Oncotarget*. 2016;7:51301-51310.

13. Ono H, Basson MD, Ito H. PTK6 promotes cancer migration and invasion in pancreatic cancer cells dependent on ERK signaling. *PLoS One*. 2014;9:e96060.

14. Ogawa K, Lin Q, Li L, et al. Aspartate beta-hydroxylase promotes pancreatic ductal adenocarcinoma metastasis through activation of SRC signaling pathway. *J Hematol Oncol*. 2019;12:144.

15. Purcell JW, Davis J, Reddy M, et al. Activity of the kinesin spindle protein inhibitor ispinesib (SB-715992) in models of breast cancer. *Clin Cancer Res*. 2010;16:566-576.

16. King RW, Jackson PK, Kirschner MW. Mitosis in transition. *Cell*. 1994;79:563-571.

17. Nurse P. Universal control mechanism regulating onset of M-phase. *Nature*. 1990;344:503-508.

18. Morla AO, Draetta G, Beach D, Wang JY. Reversible tyrosine phosphorylation of cdc2: dephosphorylation accompanies activation during entry into mitosis. *Cell*. 1989;58:193-203.

19. Jungwirth G, Yu T, Cao J, et al. KIF11 inhibitors filanesib and ispinesib inhibit meningioma growth in vitro and in vivo. *Cancer Lett*. 2021;506:1-10.

20. Talapatra SK, Schüttelkopf AW, Kozielski F. The structure of the ternary Eg5-ADP-ispinesib complex. *Acta Crystallogr D Biol Crystallogr*. 2012;68:1311-1319.

21. Lad L, Luo L, Carson JD, et al. Mechanism of inhibition of human KSP by ispinesib. *Biochemistry*. 2008;47:3576-3585.

22. Garcia PL, Miller AL, Yoon KJ. Patient-derived xenograft models of pancreatic cancer: overview and comparison with other types of models. *Cancers (Basel)*. 2020;12:1327.

23. Kapitein LC, Peterman EJG, Kwok BH, Kim JH, Kapoor TM, Schmidt CF. The bipolar mitotic kinesin Eg5 moves on both microtubules that it crosslinks. *Nature*. 2005;435:114-118.

24. Miki H, Okada Y, Hirokawa N. Analysis of the kinesin superfamily: insights into structure and function. *Trends Cell Biol*. 2005;15:467-476.

25. Castillo A, Morse HC 3rd, Godfrey VL, Naeem R, Justice MJ. Overexpression of Eg5 causes genomic instability and tumor formation in mice. *Cancer Res*. 2007;67:10138-10147.

26. Kaan HYK, Major J, Tkocz K, Kozielski F, Rosenfeld SS. "Snapshots" of ispinesib-induced conformational changes in the mitotic kinesin Eg5. *J Biol Chem*. 2013;288:18588-18598.

27. Chen G-Y, Kang YJ, Gayek AS, et al. Eg5 inhibitors have contrasting effects on microtubule stability and metaphase spindle integrity. *ACS Chem Biol*. 2017;12:1038-1046.

28. Liu C, Zhou N, Li J, Kong J, Guan X, Wang X. Eg5 overexpression is predictive of poor prognosis in hepatocellular carcinoma patients. *Dis Markers*. 2017;2017:2176460.

29. Liu M, Wang X, Yang Y, et al. Ectopic expression of the microtubule-dependent motor protein Eg5 promotes pancreatic tumourigenesis. *J Pathol*. 2010;221:221-228.

30. Sun D, Lu J, Ding K, et al. The expression of Eg5 predicts a poor outcome for patients with renal cell carcinoma. *Med Oncol*. 2013;30:476.

31. Jin Q, Huang F, Wang X, et al. High Eg5 expression predicts poor prognosis in breast cancer. *Oncotarget*. 2017;8:62208-62216.

32. Lu M, Zhu H, Wang X, et al. The prognostic role of Eg5 expression in laryngeal squamous cell carcinoma. *Pathology*. 2016;48:214-218.

33. Gomez HL, Philco M, Pimentel P, et al. Phase I dose-escalation and pharmacokinetic study of ispinesib, a kinesin spindle protein inhibitor, administered on days 1 and 15 of a 28-day schedule in patients with no prior treatment for advanced breast cancer. *Anticancer Drugs*. 2012;23:335-341.

34. Beer TM, Goldman B, Synold TW, et al. Southwest Oncology Group phase II study of ispinesib in androgen-independent prostate cancer previously treated with taxanes. *Clin Genitourin Cancer*. 2008;6:103-109.

35. Lee RT, Beekman KE, Hussain M, et al. A University of Chicago consortium phase II trial of SB-715992 in advanced renal cell cancer. *Clin Genitourin Cancer*. 2008;6:21-24.

36. Burris HA, Jones SF, Williams DD, et al. A phase I study of ispinesib, a kinesin spindle protein inhibitor, administered weekly for three consecutive weeks of a 28-day cycle in patients with solid tumors. *Invest New Drugs*. 2011;29:467-472.

37. Knox JJ, Gill S, Synold TW, et al. A phase II and pharmacokinetic study of SB-715992, in patients with metastatic hepatocellular carcinoma: a study of the National Cancer Institute of Canada Clinical Trials Group (NCIC CTG IND.168). *Invest New Drugs*. 2008;26:265-272.

38. Lee CW, Bélanger K, Rao SC, et al. A phase II study of ispinesib (SB-715992) in patients with metastatic or recurrent malignant melanoma: a National Cancer Institute of Canada Clinical Trials Group trial. *Invest New Drugs*. 2008;26:249-255.

39. Tang PA, Siu LL, Chen EX, et al. Phase II study of ispinesib in recurrent or metastatic squamous cell carcinoma of the head and neck. *Invest New Drugs*. 2008;26:257-264.

SUPPORTING INFORMATION

Additional supporting information may be found in the online version of the article at the publisher's website.